Chapter 5 Experiment

After simulation, the experiments were implemented to examine the calculation. In this chapter, the experimental instruments are introduced and the measurement results are discussed.

5.1 Instruments

5.1.1 Focused Ion Beam (FIB)

A focused ion beam (FIB) system is manipulated in a similar fashion to a scanning electron microscope (SEM) except, rather than a beam of electrons and as the name implies, an FIB system utilizes a finely focused beam of gallium ions (Ga^+) that can be operated at low beam currents for imaging or at high beam currents for milling.

The principle of an FIB system is to utilize a gallium (Ga^+) ion beam, hitting the sample surface, sputtering a small amount of material to leave the surface either secondary ions (i^+ or i^-) or neutral atoms (n^0), and producing secondary electrons (e^-), as plotted in Fig. 5.1-1. Consequently, as the Ga^+ ion beam with low current scans over the sample surface, the signal from the sputtered ions or the secondary electrons are collected to form an image; in contrast, a great deal of the material will be removed as the Ga^+ ion beam with high current bombards the sample, acting as micromachining.

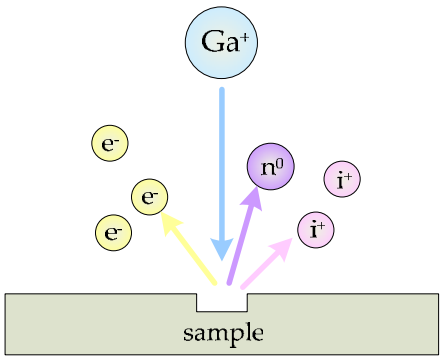

Fig. 5.1-1 Operation principle of an FIB system

Owing to the similarity of FIB and SEM, a dual-beam system that combines them on one operating platform have been commercialized and also made a great advance in analyses and manipulation at the nano-scale. The FIB instruments that we utilized are belongs to Precision Instruments Develop Center (PIDC) in Taiwan and Carnegie Mellon University (CMU) in U.S. as shown in Fig. 5.1-2.

Fig. 5.1-2 Dual beam systems (FIB/SEM) in (a) PIDC and (b) CMU

5.1.2 Near-field Scanning Optical Microscope (NSOM)

A near-field scanning optical microscope (NSOM) is to employ a subwavelength aperture in a metal sheet to scan closely over the surface of an object, and a super-resolved image can be obtained by analyzing the transmitted or reflected optical signals. In order to exploit an NSOM easily and to extend its applicability to topography, a distance regulation mechanism that is capable of automating the initial approach and maintaining the aperture at a fixed distance from the sample over the entire course of a scan is anyhow desired.

At present, a prevalent method to control the probe-sample distance relies on the utilization of a tuning folk attached to the probe, which is greatly sensitive to the shear forces arising from the interaction between the probe and the sample, as shown in Fig. 5.1-3. The information acquired by the tuning folk will be filtered and augmented by a lock-in amplifier and then transformed into a feedback signal of a

piezo-driver which controls the movement of the probe and the probe-sample distance is regulated accordingly.

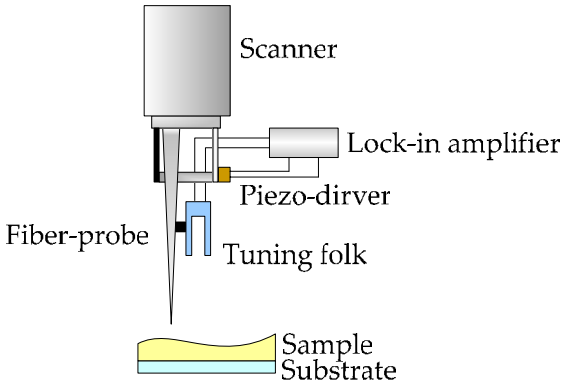

Fig. 5.1-3 Scheme of the shear force regulation mechanism

Classified by the operation modes, NSOMs can be categorized into two types: the transmission mode for a transparent sample and the reflection mode for an opaque sample, which collect the transmitted photons and the reflected photons to a photon multiplied tube (PMT) respectively; thus, both the surface topology and the near-field distribution can be obtained by analyzing the signals. The NSOMs that we exploited belong to in Academia Sinica (AS) as shown in Fig. 5.1-4.

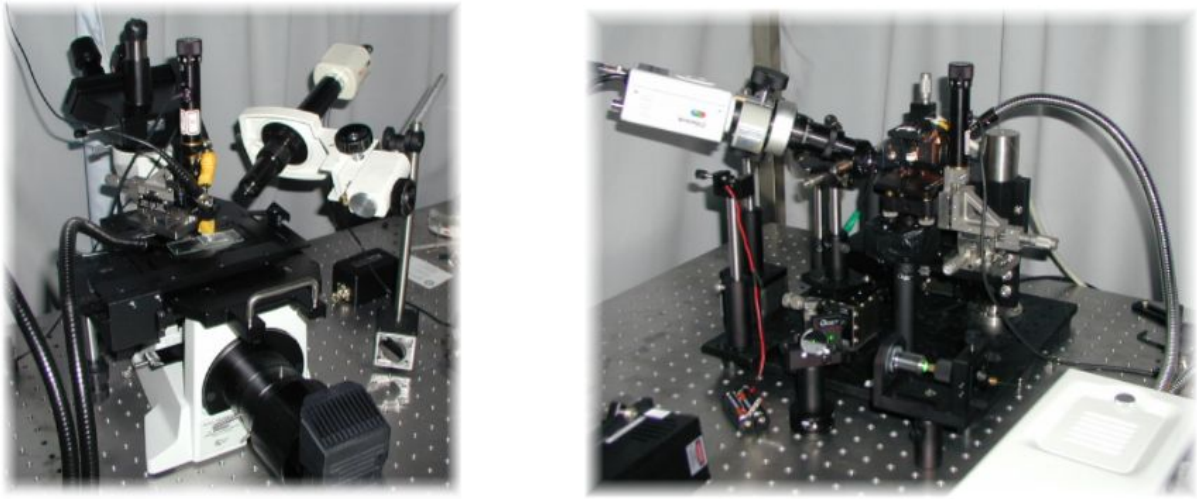

Fig. 5.1-4 NSOM in AS of (a) reflection mode and (b) transmission mode

5.1.3 Fiber-based Transmission Measurement System (FTMS)

A fiber-based measurement system that is identical to the optical model in the simulations was constructed. As illustrated in Fig. 5.1-5, the laser light of wavelength 633 nm is coupled into a single mode fiber and subsequently focused by a fiberlens. The aperture is placed at the focal plane and an objective lens is positioned behind the aperture to collect the transmitted light into a CCD camera which connects to a PC to capture the optical image of the aperture, or alternatively, a photon counter is setup to measure the transmission.

(a)

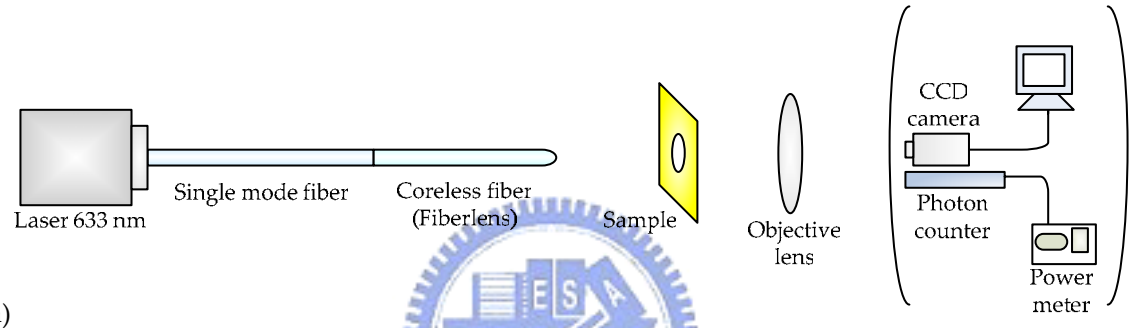

(b)

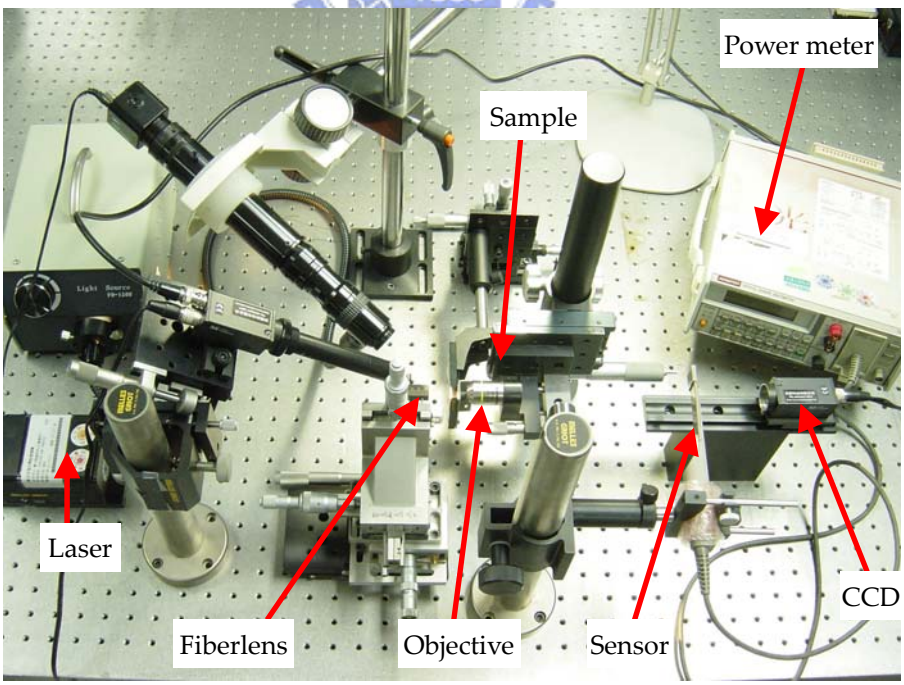

Fig. 5.1-5 (a) Scheme and (b) photo of the fiber-based transmission measurement system

5.2 Experimental Results

5.2.1 Sample Preparation

A circular aperture was prepared firstly to be a control experiment to the C-aperture. Providing a great re-produciability, the minimum line-width is 100 nm, and the circular aperture of diameter 110 nm was fabricated. Its SEM photo is shown in Fig. 5.2-1.

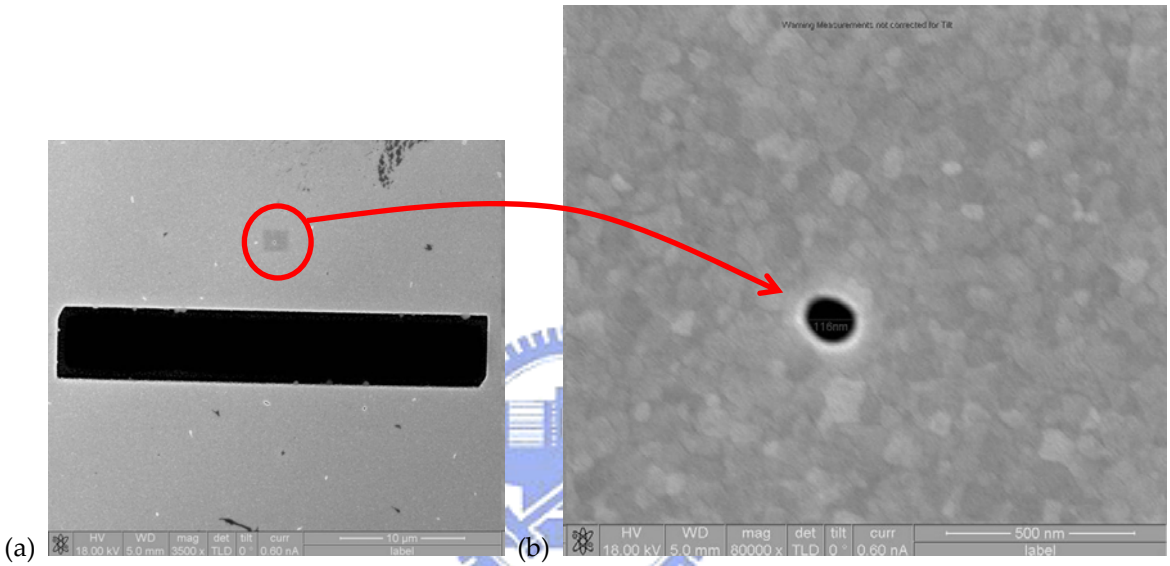

Fig. 5.2-1 SEM photos of (a) a slit as an alignment key magnified by 3500x and (b) the circular aperture with diameter of 110 nm magnified by 80000x

Limited by the resolution of FIB and re- produciability, the fabricated C-aperture shown in Fig. 5.2-2 is not exactly as the optimized one in chapter 3; however, the simulation results revealed that its power throughput would exceed over a conventional aperture by several hundreds times, which is still distinct from that of the circular aperture.

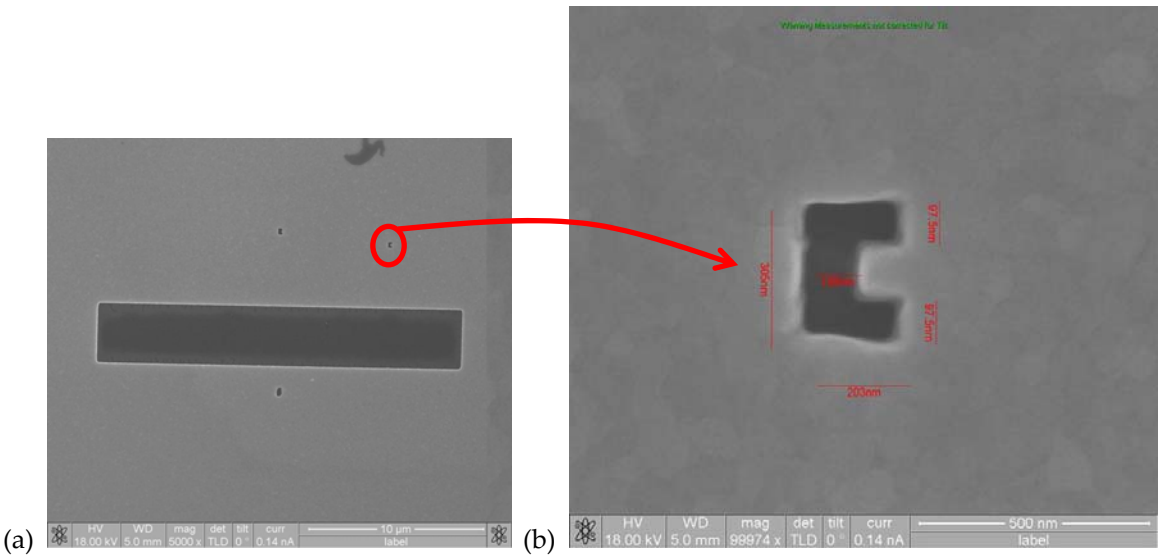

Fig. 5.2-2 SEM photos of (a) a slit as an alignment key magnified by 5000x and (b) the circular aperture with diameter of 110 nm magnified by 99974x

Finally, the single-side-corrugated C-aperture was prepared. Since the optimized groove width is much larger than the FIB resolution, it can be fabricated just as the optimized one, as shown in Fig. 5.2-3.

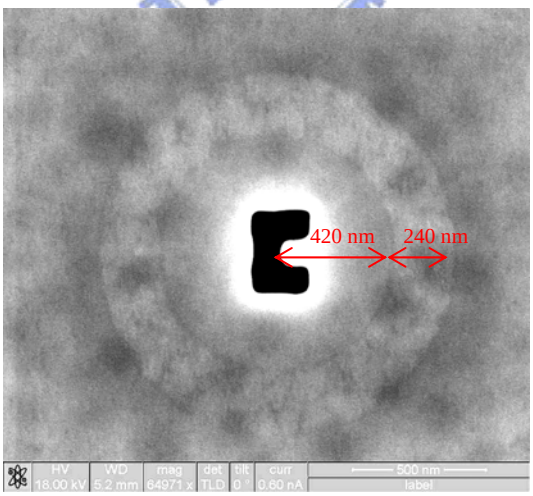

Fig. 5.2-3 SEM photo of the incident-side-corrugated C-aperture magnified by 64971x

5.2.2 Near-field Distribution

Next, the near-field distribution was obtained by means of a transmission mode NSOM. Because the transmitted energy through the circular aperture is too weak to

be recognizable from the background noise, the optical image of the circular aperture is null.

As for the C-aperture, its optical signal was detected as shown in Fig. 5.2-3, where the voltage in the scale bar is transformed from the transmitted intensity by a photo-multiplier tube (PMT). The highest background noise is 0.02 volt, and the signal through the C-aperture reaches 2 volt, indicating a signal-noise-ratio of 40 dB and demonstrating the strong transmitted optical energy through the C-aperture in comparison with the circular aperture. Additionally, because the resolution of NSOM is around 100 nm and the simulated spot size of this fabricated C-aperture is around 150*150 nm^2, the convoluted spot measured by NSOM is rationally around 300~400 nm.

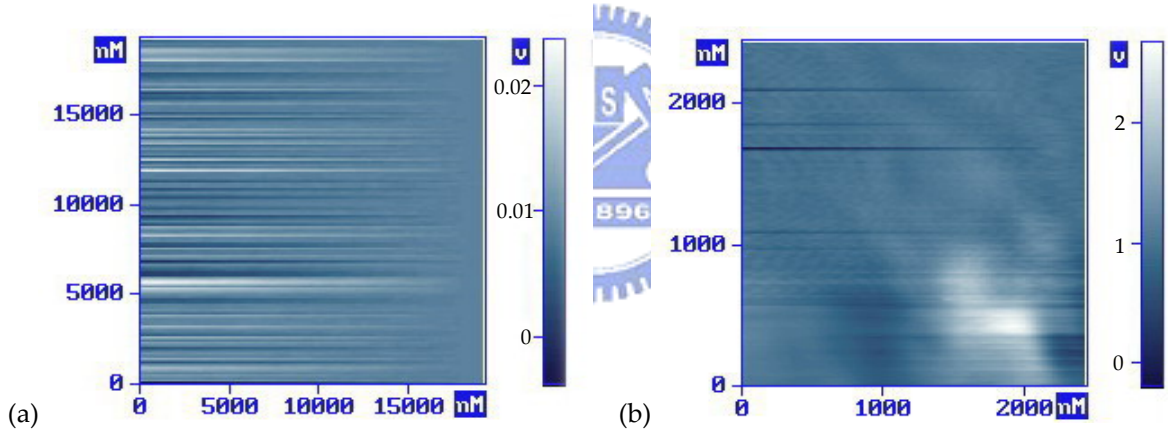

Fig. 5.2-3 Optical signal detected by NSOM of (a) background noise and (b) the C-aperture

5.2.3 Far-field Transmission

The transmission through the circular aperture and the C-aperture was then measured by a far-field apparatus. The transmission should be punctiliously manipulated so that it can be compared with the simulation results. Owing to the much larger focused spot size than the aperture size, the power throughput is proportional to the transmittance, which normalizes the transmission to the aperture area; furthermore, the transmission was the ratio of the measured power through the

aperture to that without samples. The measured and the simulated enhancements are listed in Table 5.2-1.

Table 5.2-1 Measured transmission and calculated enhancements

Sample	Circular	C-shaped	Incident-side-corrugated C-shaped
Transmission	0.01%	0.83%	1.54%
Transmittance	9.33E-03	1.66E-01	3.08E-01
Measured Enhancement (Far-field, to the circular)		***1.78E+01***	***3.30E+01***
Simulated Enhancement (Near-field, to the circular)		***1.49E+02***	***3.32E+02***

On the one hand, the C-aperture indeed increases the transmittance. Inasmuch as the transmitted intensity through the circular aperture is considerably low, the detected power is extremely affected by the ambient light, suggesting even little light leakage will cause a great noise to disturb the measurement result. Therefore, the measured transmittance of the circular aperture will be higher than the theoretical value. Furthermore, the simulated enhancements are calculated in the near-field region (several tens nanometers from the aperture) while this measurement system is operated in the far-field region (several centimeters from the aperture). As a result, the transmitted energy through the C-aperture dissipates naturally, which debases the measured enhancement; however, such a far-field enhancement of 17.8 still indicates the existence of the propagation mode. On the other hand, the incident-side-corrugated C-aperture honestly renders a further improvement in transmittance, signifying the SPP field can be coupled to the propagation mode of the C-aperture and be propagated to the far-field region. Nevertheless, both of the enhancements of 17.8 and 33.0 in comparison with the conventional circular aperture successfully demonstrate the strong near-field enhancements and suggest the great anticipation of the single C-aperture and the incident-side-corrugated C-aperture for near-field recording.

5.3 Summary

The experiments, including fabrication, near-field distribution and far-field transmission measurements were implemented and successfully demonstrated the improvements of the proposed aperture designs. Their enhancements in the transmitted energy were qualitatively confirmed; however, the further precise experiments to quantitatively examine the simulation would require amelioration in the resolution of FIB and NSOM.